

See discussions, stats, and author profiles for this publication at: <https://www.researchgate.net/publication/7108384>

Pulsed Laser Syntheses of Layer-Structured WS₂ Nanomaterials in Water

ARTICLE *in* THE JOURNAL OF PHYSICAL CHEMISTRY B · JUNE 2006

Impact Factor: 3.3 · DOI: 10.1021/jp0611471 · Source: PubMed

CITATIONS

19

READS

29

5 AUTHORS, INCLUDING:



Andrey A Voevodin

University of North Texas

241 PUBLICATIONS **6,098** CITATIONS

SEE PROFILE

Pulsed Laser Syntheses of Layer-Structured WS₂ Nanomaterials in Water

J. J. Hu,* Jeffrey S. Zabinski, Jeffrey H. Sanders, John E. Bultman, and Andrey A. Voevodin

*Materials and Manufacturing Directorate, Air Force Research Laboratory (AFRL/MLBT), Wright-Patterson Air Force Base, Dayton, Ohio 45433-7750**Received: February 22, 2006; In Final Form: March 27, 2006*

We used water as an environmental friendly medium for the synthesis of hexagonal WS₂ nanoparticles by the pulsed laser method. The materials collected on substrates were oriented with the 2H-WS₂ basal planes parallel to the surface. The use of water, UV lasers, and large WS₂ targets prevented the nanoparticles from restructuring into inorganic fullerenes, which were observed in research using hydrocarbon solvents, longer wavelength lasers, and dispersed powder targets. Fairly good dispersion of nanoparticles suggests that large surface areas are available for chemical reactivity.

Transition metal dichalcogenides, that is, MX₂, where M is Mo or W and X is S or Se, are well-known lubricants and catalysts. Their properties are determined by anisotropic layer structures (strong covalent bonding between Mo/W–S/Se but weak van der Waals attraction between lattice layers). Small-size particles of these materials have a high surface area and may form unique microstructures that can improve material properties. For example, the inorganic fullerene-like (IF) nanoparticles of MoS₂ and WS₂ were synthesized by solid–gas reactions and used effectively as solid lubricant additives for oil.^{1,2} Near-monodisperse nanofibers and nanotubules of MoS₂ were prepared by template synthesis and considered for use as hydrodesulfurization catalysts or as battery cathodes.³ Open-ended MoS₂ nanotubes produced by a solid–gas reaction were used for catalytic conversion of CO + H₂ to CH₄ + H₂O.⁴ Polycrystalline MoS₂ nanoribbon arrays produced by electrochemical/chemical synthesis were studied for electronic properties.⁵ The cost of making nanomaterials is relatively high because of the use of vacuum chambers and gas handling systems. To obtain high surface areas, highly dispersed MoS₂ materials had been synthesized by using reactions of (NH₄)₂MoS₄ in aqueous solution in the presence of an organic surfactant.⁶ High-surface-area nanostructured MoS₂ was also produced via the decomposition of (NH₄)₂Mo₃S₁₃·xH₂O in solvothermal toluene.⁷ Recently, powerful lasers have been employed to ablate materials and to prepare, at a low yield, IF-Hf₂S from HfS₃ powders in an organic solvent of *tert*-butyl disulfide.⁸ Nanotubes and nano-onions have been produced by similar methods using GaS and GaSe powders in di-*tert*-butyl disulfide/toluene/*n*-octylamine,⁹ and IF-TaS₂ was made from a pure TaS₂ pellet in liquid CS₂.¹⁰ From the large-scale manufacturing perspective, water is a preferred medium because it is environmentally friendly. Nanostructured carbons and metal colloids have been synthesized by laser ablation in water, and IF-MoS₂ nanoparticles were produced in water using an electric arc discharge.^{11–13} In this study, new layer structures and

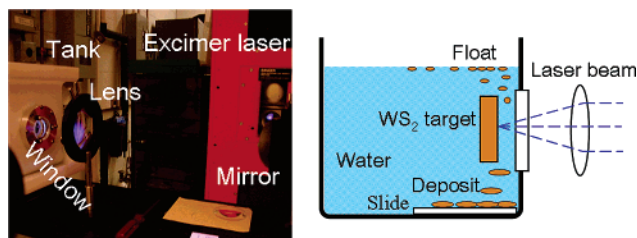


Figure 1. Experimental devices and schematic diagram of using a pulsed laser to produce WS₂ nanomaterials in water.

nanoparticles of hexagonal WS₂ were produced using pulsed laser ablation in water.

A compact disk (1 in. diameter by 1/4 in. thickness) of pure WS₂ was set in distilled water. The pulsed beam from a Lambda Physik COMPex 205 KrF excimer laser (248 nm wavelength, 20 ns duration, 1–50 Hz rate, and 200–600 mJ energy) was focused and directed through a window in front of the water tank, where the distance of the WS₂ target is about 5 mm behind the window. The syntheses occurred with 50 Hz pulses of about 400 mJ for 10–20 min. The left image in Figure 1 shows the devices used in the experiments. A schematic diagram on the right-hand side of Figure 1 shows the synthesis process, where most products of laser ablation sink in the water while some nanoparticles float on the surface because they are small and hydrophobic. The yield rate is approximately 10 mg/min. A glass slide was put on the bottom of the tank to deposit films for X-ray diffraction (XRD) measurements. Crystallographic data were collected using a Rigaku XRD system with a monochromator in front of the Cu K α X-ray source, which was operated in Θ -2 Θ mode. Standard powder XRD patterns of hexagonal WS₂ (PDF Card# 08-0237 JCPDS) were used for data interpretation. Some films floated on water, while the remainder of the laser ablated materials sunk to the bottom. The floating and sunk materials were kept separate and were collected on holey carbon grids for electron diffraction and transmission electron microscopy (TEM) analyses. High-resolution microstructures were observed using a Philips CM200-FEG transmission electron microscope operated at 200 keV, which had a field

* Corresponding author. E-mail: jianjun.hu@wpafb.af.mil.

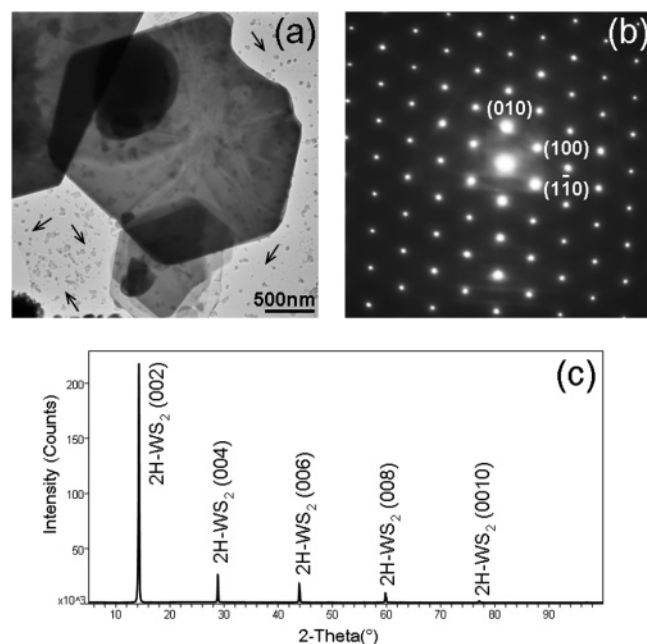


Figure 2. (a) TEM image showing WS₂ thin films and nanoparticles. (b) Selected area electron diffraction pattern of WS₂ thin films in the *c*-axis orientation. (c) XRD spectrum of the films deposited on a slide in water, which was produced by parallel basal planes of 2H-WS₂.

emission gun to provide a complete coherent electron source and nanometer-sized probe for nanostructure analyses.

The TEM observations showed that micron-sized thin films/flakes of WS₂ were produced along with a number of nanoparticles, as indicated by arrows in Figure 2a. Selected area electron diffraction patterns were indexed according to 2H-WS₂ phases with *c*-axis orientation, as shown in Figure 2b. Therefore, the normal direction of the films is parallel to the *c*-axis. The thickness of the films was measured to be less than dozens of nanometers via TEM. Considering film microstructure and thickness, it appears that pulsed laser irradiation results in the delamination and fracture of WS₂ targets at a nanometer level. Figure 2c presents the XRD spectrum of the films deposited on substrates under water, which is also indexed to 2H-WS₂. Only the (00*l*) peaks appear in the pattern because the 2H-WS₂ (002) basal planes were stacked parallel to the substrate surfaces.

The films that floated consisted of WS₂ nanoparticles, as shown in Figure 3a. They were quite evenly dispersed and exhibited little agglomeration. The nanoparticle diameters were measured to be around 10 nm, and the thickness was approximately 10 nm or less. Figure 3b and c shows the high-resolution TEM images taken from the nanoparticles, where the {100} lattices of 2H-WS₂ are directly visible. Therefore, WS₂ nanoparticles and thin films with the normal direction in the *c*-axis can be produced by pulsed laser irradiation of WS₂ targets in water. They were deposited on substrates with the basal planes lying parallel to the surface.

The mechanism of making these nanomaterials may involve two processes. The first process is laser-induced thermal shock. Stresses produced by thermal shock were not relieved by melting and would finally lead to cracking and flake detachment. This process has been termed “exfoliation” by Kelly et al.¹⁴ It is highly likely that laser exfoliation caused the delamination of nanosized layer-structured WS₂ materials. The second process follows delamination where the ejected WS₂ thin flakes and fragments were hit by shock waves produced during subsequent pulses, causing further diminution of particles. In addition, the energy of two 248 nm photons (~10 eV) is significantly higher

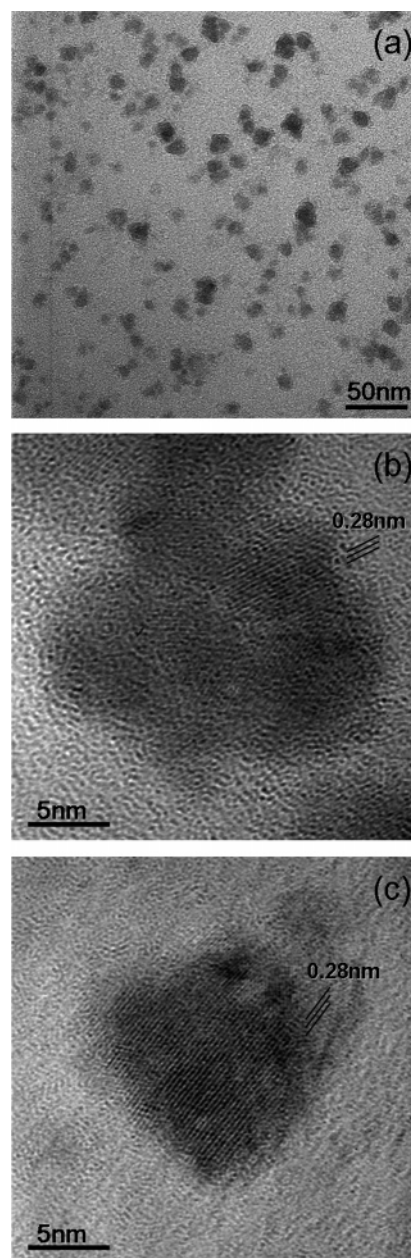


Figure 3. (a) Dispersed nanoparticles as observed by TEM. (b and c) High-resolution TEM images of nanoparticles showing the {100} lattices of 2H-WS₂.

than the dissociation and ionization thresholds of water molecules (~6.5 eV).¹⁵ Therefore, the two-photon excitation of H₂O under UV radiation leads to the generation of reactive water radicals, such as OH_{aq} and H_{aq} radicals, hydrated electrons (e_{aq}⁻), and H₃O⁺ ions.¹⁶ Those photodissociation products can act as intercalants of 2H-WS₂ materials and help the exfoliation of WS₂ in water.

Fullerene or fullerene-like structures were not detected in the present study. Their absence is likely related to the short duration of heating during the ablation/quench cycle. There were several differences compared to the previous studies: (1) Water was used as the liquid medium in place of organic/sulfide solvents, and hence, water acted as a cooling and retarding medium rather than a precursor for reaction. (2) A compact WS₂ disk was used as the laser target in place of sulfide powders/suspensions, facilitating heat dissipation in the larger solid. (3) A KrF excimer laser (248 nm) was used in place of a Nd:YAG laser (532 nm wavelength), and shorter wavelength lasers generated less

heating on the target impact. These factors acted together to preserve layered nanosized fragments instead of producing fullerene-like structures.

In conclusion, water was used as an environmental friendly medium for the synthesis of hexagonal WS₂ nanoparticles by the pulsed laser method. The use of water, UV lasers, and large WS₂ targets prevented the nanoparticles from restructuring into inorganic fullerenes, which were observed in research using hydrocarbon solvents, longer wavelength lasers, and dispersed powder targets. Fairly good dispersion of nanoparticles was observed, which suggests large surface areas are available for chemical reactivity. The materials collected on glass substrates were oriented with the 2H-WS₂ basal planes parallel to the substrate surface.

Acknowledgment. The Air Force Office of Scientific Research is gratefully acknowledged for financial support. We wish to thank Mr. A. J. Safriet and P.C. Vorum for technical assistance.

References and Notes

- (1) Tenne, R.; Margulis, L.; Genut, M.; Hodes, G. *Nature* **1992**, *360*, 444.
- (2) Rapoport, L.; Bilik, Yu.; Feldman, Y.; Homyonfer, M.; Cohen, S. R.; Tenne, R. *Nature* **1997**, *387*, 791.
- (3) Zelenski, C. M.; Dorhout, P. K. *J. Am. Chem. Soc.* **1998**, *120*, 734.
- (4) Chen, J.; Li, S.-L.; Xu, Q.; Tanaka, K. *Chem. Commun.* **2002**, 1722.
- (5) Li, Q.; Newberg, J. T.; Walter, E. C.; Hemminger, J. C.; Penner, R. M. *Nano Lett.* **2004**, *4*, 277.
- (6) Afanasiev, P.; Xia, G.-F.; Berhault, G.; Jouguet, B.; Lacroix, M. *Chem. Mater.* **1999**, *11*, 3216.
- (7) Berntsen, N.; Gutjahr, T.; Loeffler, L.; Gomm, J. R.; Seshadri, R.; Tremel, W. *Chem. Mater.* **2003**, *15*, 4498.
- (8) Nath, M.; Rao, C. N. R.; Popovitz-Biro, R.; Albu-Yaron, A.; Tenne, R. *Chem. Mater.* **2004**, *16*, 2238.
- (9) Gautam, U. K.; Vivekchand, S. R. C.; Govindaraj, A.; Kulkarni, G. U.; Selvi, N. R.; Rao, C. N. R. *J. Am. Chem. Soc.* **2005**, *127*, 3658.
- (10) Schuffenhauer, C.; Parkinson, B. A.; Jin-Phillipp, N. Y.; Joly-Pottuz, L.; Martin, J.-M.; Popovitz-Biro, R.; Tenne, R. *Small* **2005**, *1*, 1100.
- (11) Fojtik, A.; Henglein, A. *Ber. Bunsen-Ges. Phys. Chem.* **1993**, *97*, 252.
- (12) Tsuji, T.; Iryo, K.; Nishimura, Y.; Tsuji, M. *J. Photochem. Photobiol., A* **2001**, *145*, 201.
- (13) Hu, J. J.; Bultman, J. E.; Zabinski, J. S. *Tribol. Lett.* **2004**, *17*, 543.
- (14) Kelly, R.; Cuomo, J. J.; Leary, P. A.; Rothenberg, J. E.; Braren, B. E.; Aliotta, C. F. *Nucl. Instrum. Methods Phys. Res.* **1985**, *B9*, 329.
- (15) Gorner, H.; Nikogosyan, D. N. *J. Photochem. Photobiol., B* **1997**, *39*, 84.
- (16) Nikogosyan, D. N.; Oraevsky, A. A.; Rupasov, V. I. *Chem. Phys.* **1983**, *77*, 131.